Behaviour of individual VOCs in indoor environments: How ventilation affects emission from materials

Florent Caron, Romain Guichard, Laurence Robert, Marie Verriele, Frederic Thevenet

Behaviour of individual VOCs in indoor environments: how ventilation affects emission from materials

Florent Caron[1,2*], Romain Guichard[1], Laurence Robert[1], Marie Verriele[2], Frédéric Thevenet[2]

[1]French institute of research and safety (INRS), Department of Process Engineering, Rue du Morvan, 54519 Vandoeuvre-lès-Nancy, France

[2]IMT Lille Douai, University of Lille, SAGE department, 59000 Lille, France

[*]Corresponding author. E-mail address: florent.caron@inrs.fr

Abstract

Indoor air quality is affected by both emissions of Volatile Organic Compounds (VOC) from materials and ventilation. The purpose of this paper is to provide a multi-scale analysis of the impact of ventilation on VOC emissions to highlight the individual behaviours of VOCs emitted from a wood particleboard. Emissions were studied in an experimental chamber by (i) assessing the effect of ventilation on emission rates and (ii) determining intrinsic parameters (K_i, $C_{0,i}$, D_i) describing the VOC mass transfer from the material to air. The overall assessment of the effect of ventilation indicated that the air change rate could significantly affect the behaviour of individual compounds. Typically, the formaldehyde emission rate increased from 214.6 to 274.2 $\mu g.m^{-2}.h^{-1}$ when air change rate varies from 2.5 to 5.5 h^{-1}, whereas the air speed had no influence on emission rates for any VOC monitored. These results agree with the key emission parameters (partitioning and diffusion coefficients) which were higher for formaldehyde than those for other compounds. VOC diffusion related to VOC mass transfer from a material's surface to the surrounding air was the limiting step in VOC emission for the solid material studied, and should therefore be considered when developing ventilation strategies.

Keywords

ventilation ; formaldehyde ; VOC ; partitioning coefficient ; diffusion coefficient ; initial emittable concentration

1. Introduction

Modern lifestyles and climate mean that people spend more than 80% of their time in indoor environments such as public transport, the home or workplace (Zhang et al., 2012). In these environments, internal sources of emissions are the major contributors to poor air quality. Among the large variety of indoor pollutants, Volatile Organic Compounds (VOCs) are the most studied, because of their ubiquity and their indisputable negative impacts on human health (Wolkoff and Nielsen, 2001). Although the indoor concentrations of VOCs are low – in the ppb range – the exposure profile tends to be chronic. Long-term exposure to VOCs can lead to skin irritation, dizziness, and tiredness, as well as damage to pulmonary function (Yoon et al., 2010).

Among known prevention strategies, ventilation is usually recommended to reduce indoor VOC concentration. Indeed, these concentrations are simultaneously governed by both the sources of emission and the level of ventilation. Air change allows extraction and dilution to reduce the VOC concentrations from indoor sources (de Gennaro et al., 2014). However, if the ventilation is insufficient to balance indoor emissions, or if the incoming air is itself polluted, VOC concentrations tend to increase (Shang et al., 2016). To address the connection between ventilation and indoor air quality in stores, field measurement campaigns were carried out in a sports store under forced and natural ventilation conditions (Robert et al., 2018). Results indicated that, unlike other VOCs monitored, formaldehyde concentrations are not directly indexed on the ventilation condition. This result was supported by other studies, with Hun et al. (2010), Offermann and Hodgson, (2011) and Nirlo et al. (2014) reporting for equivalent real case studies showing a lack of correspondence between the concentration of formaldehyde and the air change rate (ACR). According to these references, a high ACR tends to promote VOC emissions, especially for formaldehyde, which may present a different behaviour compared to other VOCs.

Contradictory trends can also be found in the literature: in their on-site studies, Hult et al. (2015) and Huang et al. (2017) report that the formaldehyde concentration negatively

correlates with the ventilation rate. In addition, some laboratory experiments conducted under controlled conditions show that the ventilation significantly affects VOC emission rates (Knudsen et al., 1999; Myers, 1982), with the air speed over the material's surface having a marked impact (Hun et al., 2010; Knudsen et al., 1999). According to Hult et al. (2015), this effect of ventilation is related to a combination of (i) the ACR and (ii) the air velocity close to the material's surface. The influence of ventilation on the resulting VOC concentrations or directly on the VOC emission rate has not been clearly established. Given their contrasting behaviour, VOCs should be individually considered when investigating emissions from solid materials.

In addition, the mass transfers of VOCs are governed by elementary and mostly reversible mechanisms including convective mass transfer through the boundary layer, VOC diffusion within the solid material and, VOC sorption on the material's surface, which is characterized by an equilibrium between the solid material phase and the carrier gas phase (Tiffonnet et al., 2006). Consequently, VOC emissions from a solid material are controlled by a combination of diffusion within the material and mass transfer across the boundary layer in various extents (Wolkoff, 1998).

According to the literature, VOC emissions from a solid material can be described by three key emission parameters for a VOC i, at fixed temperature and relative humidity (RH) (Cox et al., 2010; Liu et al., 2013):

(i) The partitioning coefficient K_i reflects the ability of VOC i to transfer from the adsorbed phase to the gas phase according to a reversible equilibrium relationship between the material and the air

(ii) The initial emittable concentration $C_{0,i}$ ($mg.m^{-3}$) corresponds to the initial concentration of VOC i within the material that is available for emission into the surrounding air

(iii) The diffusion coefficient within the solid material D_i ($m^2.s^{-1}$) is described by the Fick's second law, considering a constant one-dimensional diffusion of VOC i in a homogeneous material

In specific ventilation conditions, the convective mass transfer coefficient h_i for VOC i may also be needed to describe mass transfer through the boundary layer. This parameter can be determined using the theoretical equation proposed by Axley (1991).

K_i, $C_{0,I}$ and D_i can be experimentally determined by adapting protocols from the literature, generally under constant temperature and RH conditions. Most published experimental protocols address each parameter independently. For example, the multi-flushing extraction method can be used to determine $C_{0,i}$ (Smith et al., 2009), whereas the porosity test method determines D_i (Xiong et al., 2008). Some experimental methods allow the two parameters to be simultaneously determined, such as the two-chamber method (Bodalal et al., 2000) and the micro-balance method (Liu et al., 2014). However, these approaches must be combined with other protocols to access the three key emission parameters. Only two methods to simultaneously determine the three parameters in a single experiment have been reported in the literature to date: (i) the C-history method (S. Huang et al., 2013) and (ii) the alternately airtight/ventilated emission method proposed by Zhou et al. (2018).

Based on the study by Tiffonnet (2000), two complementary approaches for studying VOC emission phenomena can be considered:

(i) The *chamber scale approach* monitors VOC concentration profiles emitted from a solid material placed in an experimental chamber under controlled experimental conditions. Based on the recorded profile, VOC emission rates can be calculated from the mass balance and the experimental conditions when the steady state is reached. This approach provides an overall characterization of the VOC emission process at macroscopic scale.

(ii) The *material scale approach* is based on the laws governing the mass transfer phenomenon and reflects the elementary mechanisms involved in the holistic interaction processes between a solid material and the air. The resulting VOC concentrations are expressed as a function of the physical parameters describing the state of the systems studied. Some of these parameters characterize the intrinsic proprieties of the material involved in the emission processes.

The main purpose of this paper is to address individual VOC behaviour based on a detailed analysis of the impact of ventilation on emissions of target VOCs from a typical material. The chamber scale approach was used with a reduced-scale experimental chamber to study total VOC emissions. Then, the material scale approach was used to determine the inherent characteristics of the material that directly govern VOC transfers from the material to the surrounding air. Finally, the contribution of each approach was assessed, and their interactions were determined to improve our understanding of VOC emission phenomena.

2. Materials and methods

2.1. Experimental strategy

2.1.1. Chamber scale approach

Although the impact of ventilation on VOC emissions has been widely investigated in laboratory experiments, Knudsen's group are one of the few to have highlighted an impact of air speed on VOC emissions from a solid material (Knudsen et al., 1999). However, the respective roles of the ACR and air velocity are not clearly discriminated in most experimental studies (Risholm-Sundman, 1999; Uhde et al., 1998; Wolkoff, 1998). The chamber scale approach consists in experimentally studying VOC emissions from a solid material using a ventilated experimental chamber, which allows independent control of the ACR and the air velocity over the material's surface. The resulting concentrations and emission rates for the main VOCs, including formaldehyde, can thus be determined under non-identical ventilation regimes. By discriminating between the ACR and the air velocity, it was possible to highlight and assess their respective effect on VOC emission processes.

2.1.2. Material scale approach

The two experimental protocols simultaneously determining the three key emission parameters provide equivalent accuracy and efficiency (S. Huang et al., 2013; Zhou et al., 2018). Although experiments can be carried out over reasonable time scales, the C-history method (S. Huang et al., 2013) involves many intermediate parameters and complex data processing. Consequently, fluctuating experimental data may generate extensive deviations in the results. The method proposed by Zhou et al. (2018) was therefore preferred since it involves less data processing, despite requiring more experimental abilities than the C-history method. The material scale approach used here consisted in determining the three key emission parameters for the main VOCs emitted by a solid material. The emission parameters are determined by adapting the experimental protocol developed by Zhou et al. (2018) to the experimental ventilated chamber used.

2.2. Experimental setup

2.2.1. Ventilated chamber

All experiments were carried out in a 128-L aluminium ventilated experimental chamber with inner dimensions of 0.8x0.4x0.4 m (Figure 1). The inlet and outlet ports of the chamber present circular sections with a diameter of 0.04 m, and are located on opposite faces of the chamber. The main axes of the inlet and outlet ports are located in the centre of each face, at 0.055 m from the top and 0.055 m from the bottom of the experimental chamber respectively. Flow of fresh air introduced into the chamber was controlled by BROOKS mass flow controllers, with an operation range of 0-20 $L.min^{-1}$ ± 0.25%. The fresh air from the generator contained residual impurity levels below the resolution of the analytical device. The mass balance between the inlet and the outlet was ensured by a system composed of a mass flow controller and a vacuum pump to maintain a constant outlet flow equal to the inlet flow. Given this equilibrium between the inlet and the outlet airflow, the difference of pressure between the open atmosphere and the chamber was negligible.

The air temperature in the chamber was controlled by the laboratory's temperature. This temperature is regulated by an air conditioning system set to 21 ± 0.5 °C. RH in the chamber was controlled by passing the incoming airflow through a column filled with water. The ratios of dry and water-saturated airflow rates introduced into the chamber could be adjusted to attain the desired RH. All experiments were performed at a RH of 50 ± 5 %. Temperature and RH conditions were continuously monitored using respectively a Pt 100 sensor with resolution of 0.1 °C and a capacitive sensor with resolution of 0.1 %RH from a KIMO probe placed inside the chamber.

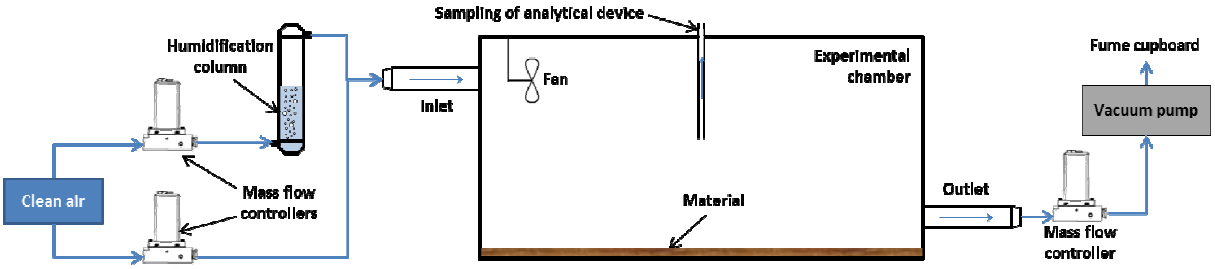

Figure 1. Experimental setup showing the 128 L aluminium ventilated chamber.

A mixing fan was placed close to the ceiling of the chamber and oriented in the direction of the main axis of the inlet flow at 0.1 m from the inlet port. This fan, measuring 127x127x38 mm, generated an airflow of 270 $m^3.h^{-1}$ at a nominal voltage of 12 V. The ACR was controlled by mass flow controllers, whereas the mixing fan regulated mixing of the air inside the experimental chamber.

2.2.2. Selected material

The sample used for this paper was a commercial wood particleboard (PB) with a waterproof coating, considered a model material. This material was chosen for its simple geometry, the diversity of VOCs it emits, and its wide use in indoor environments as well as because many studies have examined VOC emissions from construction materials. The 0.015-m-thick wood panel measuring 0.795x0.395 m was placed inside the experimental chamber with only one face of the panel exposed. PBs from the same batch were used for each series of tests. All

179 panels were packaged in plastic film and stored in a light-protected area in the air-
180 conditioned laboratory to avoid any VOC depletion as a result of passive emissions into the
181 air.

182 **2.2.3. VOC monitoring**

183 The diversity of C6 – C16 VOCs and carbonyl compounds emitted from the PB in the air
184 chamber was initially screened using off-line measurement methods. To do so, air samples
185 were collected from the chamber onto DNPH and TENAX sorbent cartridges. DNPH
186 cartridges were desorbed with acetonitrile and analysed using an UltraViolet – High
187 Performance Liquid Chromatography (UV-HPLC) system. TENAX sorbent cartridges were
188 thermally desorbed and analysed using a Thermal Desorption-Gas Chromatograph equipped
189 with Flame Ionization and Mass Spectrometer detectors (TD/GC-FID-MS). Chromatographic
190 analyses revealed that the main VOCs emitted from the PB were: acetone, acetaldehyde,
191 formaldehyde, propanal, butanal, pentanal, hexane and mono-terpenoid compounds
192 including α-pinene, β-pinene, limonene, 3-carene, camphene, and α-phellandrene. These
193 VOCs were therefore specifically monitored in subsequent experiments.

194 Throughout the emission vs. ventilation experiments, VOCs were monitored using an online
195 Selected Ion Flow Tube – Mass Spectrometer (SIFT-MS). This instrument relies on the
196 positive chemical ionization technique, but does not require specific sample preparation or
197 pre-concentration. First, ions are formed by microwave discharge on wet air at low pressure.
198 A first quadrupole alternatively selects H_3O^+, NO^+ and O_2^+ ions. Selected ions and analytes
199 then enter the flow tube, where specific product ions are formed and separated according to
200 their mass-to-charge ratio (m/z). These products are detected using a second quadrupole.
201 Concentrations were calculated after calibration based on the signal intensity of each VOC
202 with a resolution of 1 ppb. The limits of detection (LoD) of our analytical procedure were
203 calculated from blank measurements, and are reported in Table 1. The reagent ions and
204 product ions monitored for this study are listed in Table 1 for each VOC monitored. Since the
205 principle of the mass spectrometry detector is to separate compounds according to their

mass, the mass resolution of the SIFT-MS device cannot discriminate between the different mono-terpenes emitted from the wood PB. “Terpene” was therefore hereafter used to designate all emitted terpenoid VOCs.

Table 1. Reagent ions and specific ions used to monitor VOCs emitted from the PB.

VOC	Formaldehyde	Acetone	Acetaldehyde	Propanal	Butanal	Pentanal	Hexanal	Terpenes
Reagent ion	H_3O^+	NO^+	NO^+	NO^+	NO^+	NO^+	NO^+	NO^+
Specific ion	CH_3O^+	$NO^+.C_3H_6O$	CH_3CO^+	$C_3H_5O^+$	$C_4H_7O^+$	$C_5H_9O^+$	$C_6H_{11}O^+$	$C_{10}H_{16}^+$
m/z	31	57	43	57	71	85	99	136
LoD (ppb)	20	37	28	2	1	1	26	6

Before placing the PB in the experimental chamber, the chamber was flushed with fresh air, and blank measurements were taken to determine the background VOC concentrations. SIFT-MS VOC monitoring started as soon as the material was placed inside the experimental chamber. An airflow rate of 25 mL.min^{-1} was continuously sampled from the centre of the chamber by the analytical device. The volume of gas sampled throughout emission experiments was typically less than 6% of the volume of the experimental chamber, and thus gas sampling was assumed not to affect the emission equilibrium.

2.2.4. Aeraulic characterization of the chamber

Ventilation can be characterized by two aspects: the ACR and the air velocity near to the material’s surface.

The ACR corresponds to the rate at which indoor air is renewed by incoming fresh air. It is expressed as a number of volumes per hour (h^{-1}). The ACR in our ventilated chamber, with an operation range of 0 - 18.75 h^{-1}, was controlled by two BROOKS mass flow regulators.

The air velocity near to the material’s surface is defined in the direction of the airflow along the PB. Air velocity profiles near the material’s surface had to be investigated and determined. Air velocities were measured using a TSI hot wire anemometer probe placed 0.5 cm above the surface of the PB; it had a resolution of 0.01 m.s^{-1}. First, the airflow was

established inside the chamber after replacing one of the lateral sides of the chamber by a wooden panel drilled at several points at the relevant distance from the bottom of the chamber to allow the probe insertion. The end of the probe was oriented in the direction of the airflow, parallel to the surface of the material to be measured. Air velocity measurements using the anemometer probe were performed in 15 separate locations above the material's surface as shown in Figure 2-a. The air velocity profiles determined were then used to calculate an average air velocity at the surface of the material under various air mixing conditions. Figure 2-b presents an example of an air velocity profile near to the material's surface. This profile is the result of measurement of five average air velocities near to the material's surface: 0; 0.5; 1.0; 1.4, and 1.8 $m.s^{-1}$. Note that the ACR has no effect on the air velocity over the material's surface. Consequently, only the fan used to mix the air inside the chamber controls the air velocity over the material's surface.

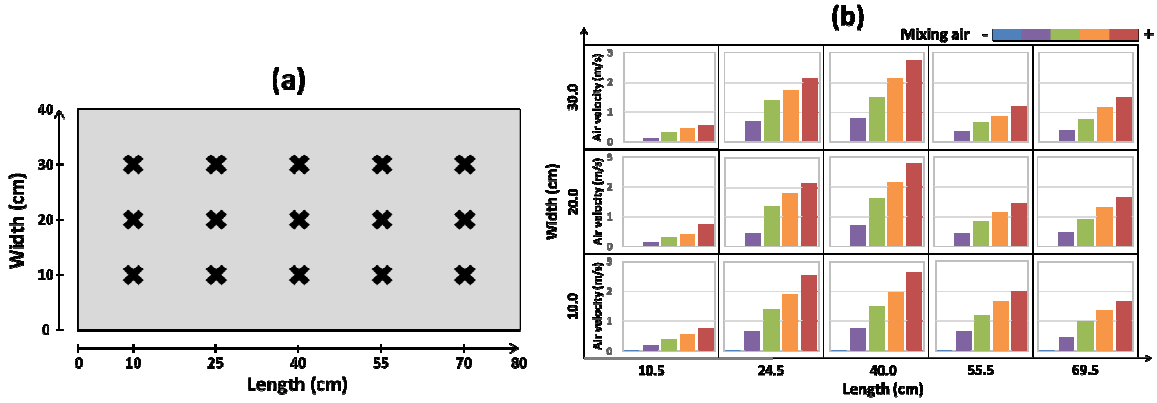

Figure 2. (a) Top view schematic representation of the material surface, crosses represent locations where air velocity was measured, (b) example of air velocity profile near to the material's surface as a function of air mixing at a constant ACR of 3.5 h^{-1}.

2.3. Experimental protocol for the chamber scale approach

2.3.1. Characterizing the effect of ventilation on VOC emission rates

To assess the effect of ventilation, it was necessary to examine how: (i) the air velocity near to the material's surface, and (ii) the ACR affected emission rates for the VOCs emitted from the PB at 21 °C and 50% RH.

The first series of experiments assessed how the air velocity near to the material's surface affected emission rates for the main VOCs. An ACR of 4.5 h^{-1} was set and the average air speeds over the material's surface tested were: 0; 0.5; 1.0; 1.4, and 1.8 $m.s^{-1}$ without changing the PB sample. The second series of tests assessed the impact of the ACR on emission rates for the main VOCs monitored. The average air velocity near to the material's surface was 0.5 $m.s^{-1}$, whereas the ACR was set to: 2.5; 3.5; 4.5, or 5.5 h^{-1}. The PB sample was changed between experiments.

The VOC concentration gradient between the material's surface and the ambient air was monitored over time to allow VOC emission rates to be considered and compared under equilibrated conditions. Therefore, after loading the PB into the experimental chamber, concentrations were allowed to stabilize until changes no longer exceeded the corresponding measurement uncertainty. At this stage, the VOC dynamic equilibrium between the gas-phase and the material's surface was considered have been reached. Thus, the concentration of a given VOC at the dynamic equilibrium corresponds to the steady state concentration. The emission rate was deduced from this steady state concentration for VOC i, the ACR and the loading factor, as described in Equation 1. The steady state concentration corresponds to the average concentration measured over 20 min at least 1 h after reaching the VOC emission equilibrium.

$$E_i = N C_{ss,i} / L \quad (Equation\ 1)$$

In Equation 1, E_i is the emission rate for VOC i ($\mu g.m^{-2}.h^{-1}$), N is the ACR (h^{-1}), $C_{ss,i}$ is the steady state concentration of VOC i ($\mu g.m^{-3}$) and L is the loading factor for the emissive material ($m^2.m^{-3}$), which corresponds to the ratio between the exposed surface area (m^2) and the air volume (m^3).

2.3.2. Characterizing variability between PB samples

The PB samples used for each series of tests were from the same batch, but as the manufacturing process could introduce variability between PB samples, it was nevertheless

necessary to assess their heterogeneity. Heterogeneity between samples was assessed based on variations in the individual VOC emission rates between three samples; it was expressed as a standard deviation value. For these purposes, three experiments were performed at 21 °C, 50% RH and at an ACR of 4.5 h^{-1}, changing the PB sample between experiments.

2.3.3. Characterizing VOC depletion from the PB

The chosen material acts as a source of VOCs throughout the all experiments, since mass transfer for the VOC occurs continuously from the solid bulk material to the air. Under ventilated conditions, gas-phase VOC concentrations at dynamic equilibrium tended to decrease gradually as a result of VOCs present in the solid material becoming depleted over time as a result of emission, since they are present in the material in finite quantities. This process is called material depletion and can be characterized by a depletion rate, k_d^i expressed in h^{-1}.

Material depletion was assessed by performing a series of six consecutive, identical experiments with a single PB at an ACR of 4.5 h^{-1} under constant temperature (21 °C) and RH (50%). The PB was removed from the chamber and stored under plastic film between tests while flushing the chamber with fresh air. In each consecutive experiment, the VOC concentrations were determined once the steady state had been reached. The concentration profiles obtained in these experiments could be described as an exponential decay from which the depletion rate for a given VOC i k_d^i can then be determined.

2.3.4. Characterizing the temperature effect

According to Wolkoff (1998), temperature affects the emission rate for some VOCs but this temperature effect strongly depends on the type of material and the nature of the emitted VOC. According to the statistical analysis proposed by Liu et al. (2014), VOC emissions increased significantly at high temperature, as shown by the good agreement between the model-predicted concentration, based on diffusion within the solid material, and the gas-

300 phase concentration measured. In contrast, Huangfu et al. (2019) clearly highlighted a linear
301 relationship between the formaldehyde concentration over a 20 to 45 ppb range and an
302 indoor air temperature ranging from 19 to 24 °C.

303 Based on these observations, the influence of temperature on VOC emissions must be
304 assessed. The effect of temperature on VOC emissions was examined in the steady state
305 concentration regime under airtight conditions with a single material plate in conditions
306 guarding against VOC depletion from the material, and to limit variability between samples.
307 In these experiments, five temperatures from 19 to 28 °C were tested in a random order, by
308 changing the temperature of the inlet air and the laboratory temperature after emissions had
309 reached the steady state.

310 From this experimental assessment, a relationship linking VOC concentrations under airtight
311 conditions to temperature was determined. The influence of temperature on the VOC
312 concentrations can be then characterized by the relative concentration enhancement of VOC
313 i per degree Celsius, as described By Equation 2.

314 $$\alpha_i = \frac{C_i(T_{max}) - C_i(T_{min})}{(T_{max} - T_{min})C_i(T_{ref})} \quad (Equation\ 2)$$

315 Where C_i is the concentration of VOC i at a fixed temperature (ppb), T_{max} is the maximum
316 temperature in the range (°C), and T_{min} is the minimum temperature in the range (°C).

317 **2.4. Experimental protocol for the material scale approach**

318 **2.4.1. Principle of the experimental method used to determine the emission**
319 **parameters: K_i, $C_{0,i}$ & D_i**

320 The principle of the method proposed by Zhou et al. (2018) is based on the alternation of two
321 states: (i) *VOC emissions monitored under airtight conditions* and, (ii) *VOC emissions*
322 *monitored under ventilated condition*.

323 In the first step, VOCs are emitted from the solid material of interest, placed in a clean
324 experimental chamber, under airtight conditions, constant temperature, and RH. The source

material is left inside the experimental chamber until the emission equilibrium is reached for every VOC. The concentration of VOC i at equilibrium in the airtight container, expressed in $mg.m^{-3}$, corresponds to the average concentration measured over 20 min at least 1 h after reaching the VOC equilibrium between the gas-phase and the material's surface. Fresh air was then introduced into the experimental chamber at a constant airflow rate, with an ACR set to 2.35 h^{-1} to mark the beginning of the second step: monitoring of VOC emissions under ventilated conditions. When all VOC concentrations in the chamber had once again reached a concentration equilibrium, the ventilated step was considered finished and the setup was returned to the airtight condition. The solid material was subjected to a total of five airtight conditions and four ventilated conditions as reported in Figure 3. To assess the repeatability of this experimental method, three full experimental sequences were performed under the same experimental conditions.

As illustrated in Figure 3, different VOCs emitted from the same material may exhibit distinct individual emission kinetics, especially under airtight conditions. Some VOCs can reach their steady state equilibrium within only 3-4 h, while others may need more than 10 h. These contrasting emission kinetics generate a time constraint when establishing the steady state in each experimental phase for all VOCs. Therefore, it was necessary to wait at least 10 h under airtight conditions to ensure that all VOCs had reached their respective steady states. The steady state for a given VOC is reached when the measured concentration of that VOC does not vary beyond its measurement uncertainty for a minimum of 20 min.

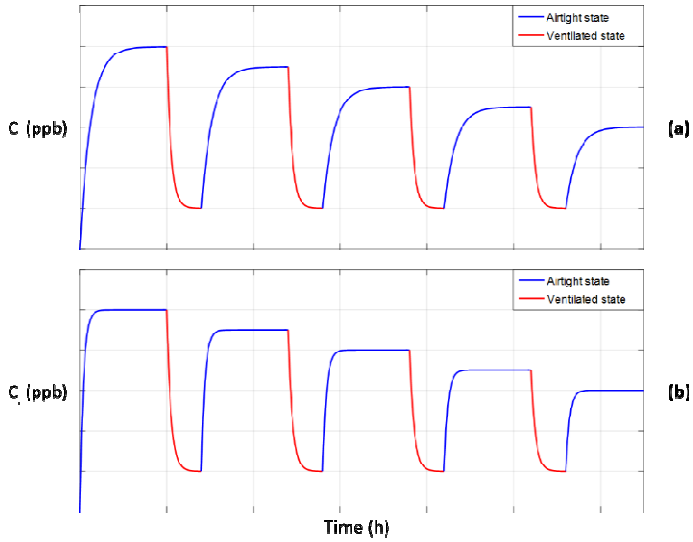

345

346 **Figure 3. Theoretical plots of the successive emission states: (a) gas concentration (ppb) of**
347 **VOC i illustrating a slow kinetic emission as a function of time; (b) gas concentration (ppb) of**
348 **VOC j illustrating a rapid kinetic emission as a function of time.**

349 During the ventilated phases, the nature of the VOCs did not significantly influence the time
350 required to reach the steady state because fresh air was constantly passing through the
351 system. To ensure all VOCs have reached their steady state, it was necessary to wait from 4
352 to 5 h under ventilated conditions. Note that the VOC concentration was considered to be at
353 the steady state if it remained unchanged beyond the measurement uncertainty for at least
354 one hour.

355 ### 2.4.2. Determining K_i and $C_{0,i}$ from experimental data by linear fitting

356 After performing the multiple airtight and ventilated protocols, the concentration of VOC i
357 reached at equilibrium during each airtight step and the total mass of VOC i emitted during
358 ventilated periods were determined from the temporal concentration profiles for each VOC
359 (Figure 3). For each ventilated state, the mass of VOC i emitted, expressed in mg, was
360 calculated using the trapezoidal quadrature formulae.

361 Henry's law describes the transient and reversible equilibrium relationship between the gas
362 phase concentration at equilibrium and the adsorbed phase concentration on the solid
363 material. Based on this law, the general VOC mass balance inside the chamber for the

multiple airtight/ventilated emission states was used to develop the relationship between the VOC concentration at equilibrium and the mass of VOC emitted, including the partitioning coefficient and the initial emittable concentration. The general mass balance equation can be found in original publication of Zhou et al. (2018). Finally, the partitioning coefficient K_i and the initial emittable concentration $C_{0,i}$ were obtained for VOC i from the linear fitting of multiple sets of VOC concentrations at equilibrium, and the mass of VOC i emitted.

2.4.3. Determining D_i by solving analytical equations

In addition to K_i and $C_{0,i}$, the diffusion coefficient D_i, expressed in $m^2.s^{-1}$, must be determined for VOC i. This parameter is calculated by non-linear fitting of the first experimental curve for airtight emission and analytical resolution of the equation of gas-phase VOC concentrations in an airtight chamber using the K_i and $C_{0,i}$ values determined previously, as proposed by Xiong et al. (2011).

When characterizing the mass transfer for VOC i, the Biot number is included in the equation of the gas-phase VOC concentration in an airtight chamber. The Biot number corresponds to the ratio between the mass transfer inside the material and the mass transfer at the material's surface; therefore, the convective mass transfer coefficient h_i through the boundary layer at the surface-air interface for each VOC i, expressed in $m.s^{-1}$, is included in the equation. According to Axley (1991), the convective mass transfer coefficient h_i for VOC i can be theoretically calculated by applying Equation 3. This equation includes the Reynolds number and the Schmidt number, described by Equation 4 and Equation 5, respectively.

$$\frac{h_i L}{\delta_i} = 0.664 Re^{1/2} Sc^{1/3} \quad (Equation\ 3)$$

For Re < 500,000

$$Re = \frac{UL}{\nu} \quad (Equation\ 4)$$

$$Sc = \frac{\nu}{\delta_i} \quad (Equation\ 5)$$

Where *Re* is the Reynolds number, *Sc* is the Schmidt number, δ_i is the molecular diffusivity of VOC i in air outside the boundary layer ($m^2.s^{-1}$), *U* is the mean air velocity outside the boundary layer ($m.s^{-1}$), *L* is the length of the surface in the direction of airflow (m) and *v* is the kinetic viscosity of the air phase ($m^2.s^{-1}$).

2.4.4. Method to estimate the molecular diffusivity of VOC i in air

Calculation of the convective mass transfer coefficient, h_i, for VOC i depends on the experimental conditions and on the molecular diffusivity coefficient of VOC i. This value must therefore be individually determined for each VOC. However, molecular diffusivity coefficient values were found for five VOCs in the GSI chemical database, except for pentanal, hexanal, and terpenes. Among the chemical property estimation methods present in the literature, the method proposed by Fuller et al. (1969) can be used to estimate the molecular diffusivity coefficient of a binary gas-phase system based on the molar weight and the atomic diffusion volume (Fuller et al., 1969, 1966; Fuller and Giddings, 1965). Based on an empirical relationship proposed by Fuller et al. (1969), Equation 6 was modified to estimate the molecular diffusivity coefficient δ_i for a given VOC i in air.

$$\delta_i = \frac{0.01\,T^{1.75}(1/M_i + 1/M_{air})^{1/2}}{P\left[(\sum v)_i^{1/3} + (\sum v)_{air}^{1/3}\right]^2} \quad (Equation\ 6)$$

In Equation 6, δ_i is the molecular diffusivity coefficient of VOC i in air ($m^2.s^{-1}$), *T* is the temperature (K), *P* is the pressure (Pa), M_i is the molar weight of VOC i ($g.mol^{-1}$), M_{air} is the molar weight of air ($g.mol^{-1}$) and $\sum v$ is the sum of atomic diffusion volume increments (cm^3). The atomic diffusion volume increments were determined by performing regression analysis on extensive experimental data and are reported in Fuller et al. (1969).

3. Results and discussion

The following sections present the results of the study split into two main parts. The first part focuses on the chamber scale investigation with the prior assessment of VOC emission variability and the assessment of the influence of ventilation on VOC emissions. The second

413 part focuses on the material scale investigation, presenting the emission parameters
414 describing the VOC mass transfer.

415 ### 3.1. Chamber scale investigation

416 #### 3.1.1. Assessing emission variability

417 Before assessing the influence of ventilation on VOC emissions, it was necessary to
418 determine the variability of VOC emissions, including (i) variability between samples, (ii)
419 depletion of VOC from the material studied, and (iii) the influence of temperature on VOC
420 emissions.

421 #### 3.1.2. Variability of emission rates between samples

422 Emission variability was assessed by determining the standard deviation of the emission
423 rates measured for three PB samples. For every VOC monitored and for the three PB
424 samples, Table 2 lists the emission rates followed by the measurement uncertainties. The
425 standard deviation related to the variability of the emission rate between samples was
426 calculated for all VOCs.

427 **Table 2. Emission rates of VOCs ($\mu g.m^{-2}.h^{-1}$) and associated standard deviations (SD)**
428 **determined from three series of experiments performed under the same conditions.**
429 **Uncertainties correspond to the SD calculated from the concentrations measured.**

E_i ($\mu g.m^{-2}.h^{-1}$)	Formaldehyde	Acetone	Acetaldehyde	Propanal	Butanal	Pentanal	Hexanal	Terpenes
Sample 1	223 ± 12	2887 ± 170	125 ± 14	18.3 ± 1.7	8.0 ± 1.0	17.0 ± 1.4	1082 ± 58	226 ± 16
Sample 2	256 ± 14	3265 ± 193	141 ± 16	17.2 ± 1.6	8.0 ± 1.0	19.0 ± 1.5	1248 ± 67	305 ± 21
Sample 3	234 ± 13	3214 ± 190	133 ± 15	17.2 ± 1.6	8.0 ± 1.0	19.0 ± 1.5	1209 ± 65	348 ± 24
SD	16.9	205.1	7.7	0.6	0.1	1.1	86.8	62.3

430 As reported in Table 2, the SD reflecting the variability of emission rates between PB
431 samples from the same batch were less than 8%, except for terpenes, which has a 21.3%
432 SD. The SD for formaldehyde, acetone, terpenes, and hexanal were all higher than the
433 corresponding measurement uncertainties. The amounts of these VOCs present in the PB
434 samples from the same batch presented a slight variability between samples. SD for
435 acetaldehyde, propanal, butanal, and pentanal were lower than the measurement

uncertainties. The amounts of these VOCs into the PB samples can therefore be regarded as homogeneous.

3.1.3. Contribution of natural depletion

The characterization of VOC depletion from the material based on a series of six consecutive experiments on a single PB under identical experimental conditions is illustrated by the terpene concentration plotted over time, i.e. the depletion profile for terpenes, shown in Figure 4.

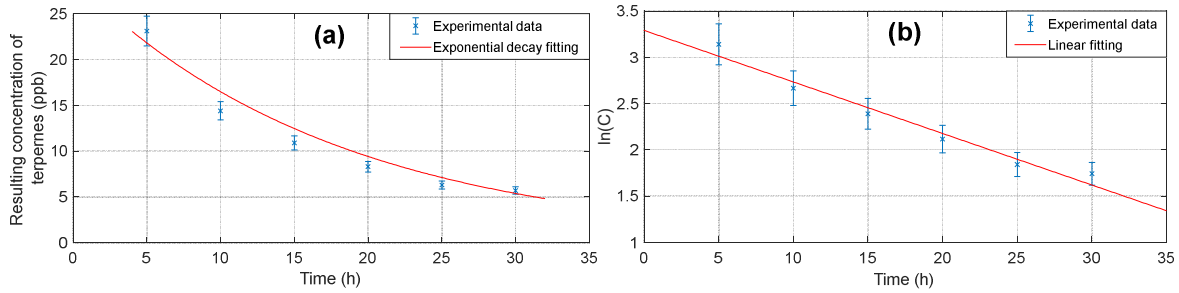

Figure 4. (a) Terpene depletion profile determined from six consecutive experiments. (b) Linearized depletion profile for terpene. Uncertainties correspond to the standard deviation calculated from the concentrations measured. (T = 21 ± 0.5 °C, RH = 50 ± 5%, ACR = 4.5 h^{-1}, surface air velocity = 0.5 $m.s^{-1}$).

Like this terpene depletion profile (Figure 4-a), all monitored VOCs followed an exponential decay profile that could be described with first order kinetics. These temporal profiles are in agreement with findings reported by Harb et al. (2018). Depletion rates expressed in h^{-1}, were retrieved, for each VOC from the slope of the linearized temporal profiles (Figure 4-b).

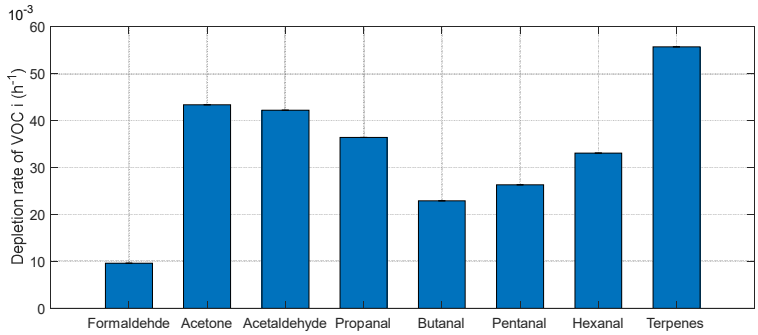

Figure 5. Depletion rates for the eight VOCs monitored in the selected PB (h^{-1}).

All VOCs were characterized by depletion rates within the same order of magnitude (Figure 5). The lowest value was recorded for formaldehyde at 9.6 x 10^{-3} h^{-1}, whereas other VOCs presented depletion rates exceeding 22.9 x 10^{-3} h^{-1}. Considering the depletion rates measured for all VOCs, the VOC depletion of the PB is less than 2% over the 20 min required to determine the steady state concentration.

The depletion rates reported here are one order of magnitude higher than those reported in Harb et al. (2018). This apparent discrepancy is probably mainly linked to differences in ventilation conditions. Indeed, we used an ACR of 4.5 h^{-1} in our experiments; whereas Harb et al. (2018) used a lower ACR of 0.3 h^{-1}. The flushing of the air volume by the higher ACR increases the concentration gradient between the material's surface and the air. Therefore, with a higher ACR, mass transfer of VOC from the material to the air increases due to the larger concentration gradient, and consequently the VOC is more rapidly depleted from the material.

As the material depletion was significant over the timespan of the experiments investigating the influence of ventilation on VOC emission rates, the VOC concentration profiles obtained should be corrected using the depletion rate determined as detailed in Harb et al. (2018), using Equation 7.

$$C^i_{corr} = exp\left[\ln\left(C^i\right) + \left(k^i_d t\right)\right] (Equation\ 7)$$

Where C^i_{corr} is the corrected VOC i concentration (ppb), C^i is the measured VOC i concentration (ppb), k^i_d is the depletion rate for VOC i (h^{-1}) and *t* is the time along the consecutive series of experiments (h).

3.1.4. Effect of temperature on VOC concentrations

The effects of temperature on the concentration of a given VOC are illustrated in Figure 6-a for formaldehyde. Uncertainties correspond to the SD calculated from the monitoring of

steady state concentrations. For each VOC, Figure 6-b shows the relative concentration enhancement per degree Celsius.

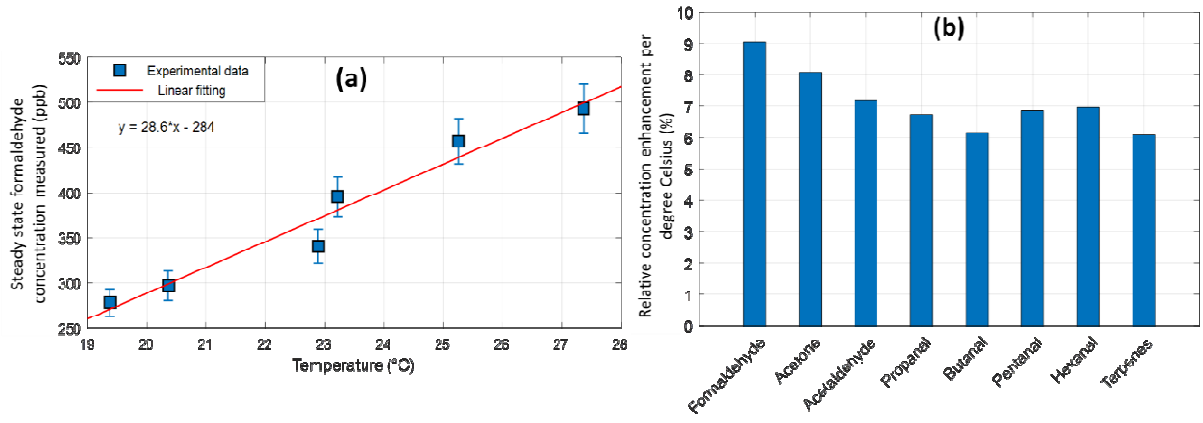

Figure 6. (a) Steady state concentration of formaldehyde (ppb) as a function of chamber temperature (°C); (b) Relative concentration enchancement per degree Celsius (%) for each VOC monitored.

As illustrated in Figure 6-a for formaldehyde, all VOCs presented a linear relationship between their steady state concentrations and the temperature in the chamber under airtight conditions over the temperatures range 19 to 28 °C. The sensitivity of VOC concentrations to temperature is represented by the relative concentration enhancement per degree. According to Figure 6-b, all VOCs were temperature-sensitive, with relative concentration enhancements between 6 and 9 %.

The sensitivity of VOC emissions to temperature underscores the need to consider this parameter when setting up experimental tests, especially under unstable temperature conditions. From the relative concentration enhancement parameter (Equation 2), the concentration datasets can be corrected for temperature when the temperature fluctuates during experiments. However, it is not always necessary to correct data with respect to temperature, and VOC concentrations should only be corrected when large temperature variations occur, particularly in long-term experiments.

According to the literature, the effect of RH on VOC emissions does not show any particular trends. Indeed, authors report a variable influence of RH on VOC emissions depending on

499 the VOC-material system considered (Colombo et al., 1993; L. Huang et al., 2013; Wolkoff,
500 1998). When studying VOC emissions at different RH conditions, it appears required that
501 selected materials undergo preliminary conditioning at the targeted RH to equilibrate the
502 material surface and bulk to the corresponding RH before initiating any test. This preparation
503 aims to avoid material absorption/release of moisture and maintain constant RH along
504 experimental tests. Evaluating the effect of RH is complex since the material preparation may
505 induce VOC depletion resulting in VOC emissions from the material. During experiments,
506 variations in RH may affect the emission data obtained. Therefore, along our experiments,
507 the RH remains constant in order not to bias any emission process.

508 **3.1.5. Influence of ventilation on VOC emission rates**

509 The chamber scale approach allowed us to study the effect of ventilation on VOC emission
510 rates from the selected PB. The roles of air velocity over the material's surface and ACR
511 were dissociated. Their respective influence on VOC emission rates were investigated and
512 are reported in this section.

513 **3.1.6. Specific influence of air velocity over the material surface on VOC**
514 **emission rates**

515 The impact of changes in the air velocity near to the material's surface on VOC emissions
516 from PB was studied by determining the emission rates for VOCs when applying different air
517 velocities over the material's surface at a constant ACR. The corresponding data are
518 reported in Figure 7. Since a single material sample was used for this series of tests,
519 datasets were corrected to account for VOC depletion, assuming a constant depletion rate
520 over the series of tests.

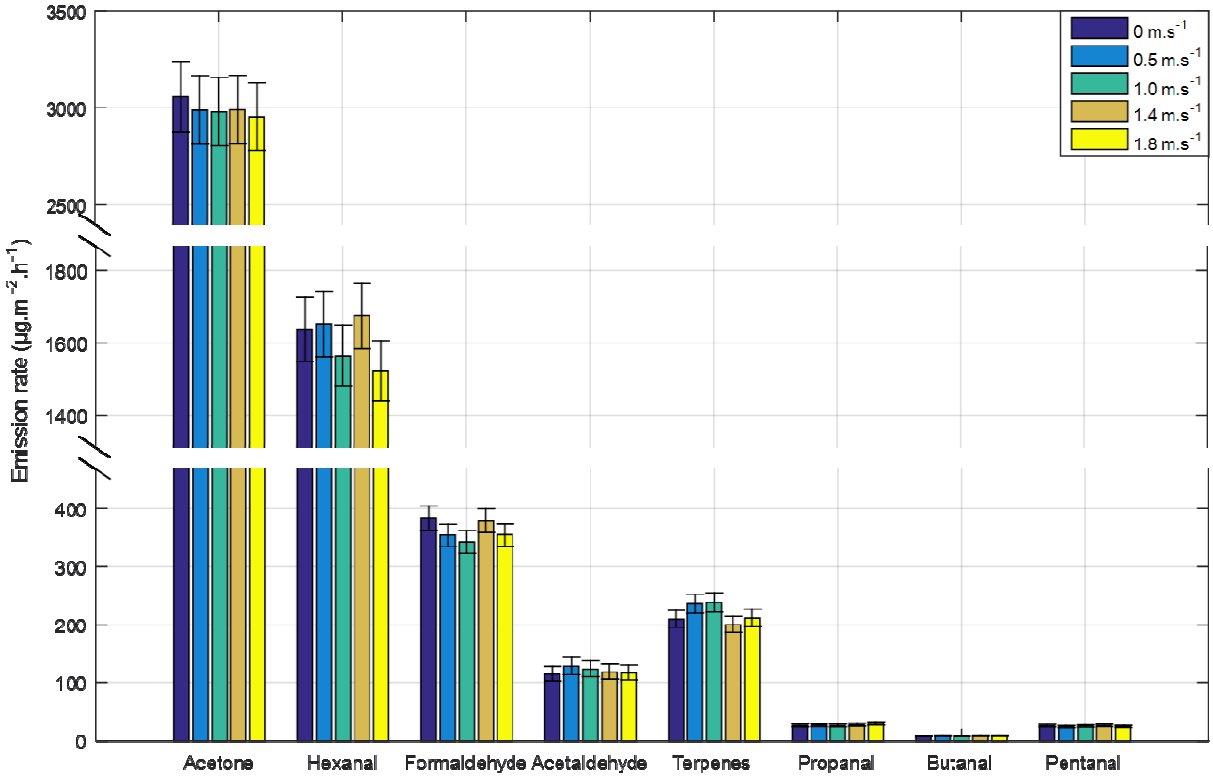

Figure 7. Emission rates (µg.m^{-2}.h^{-1}) for the eight main VOCs when applying different air velocities near to the material's surface (m.s^{-1}). Uncertainties correspond to the standard deviation calculated from the steady state concentrations measured.

Among the VOCs monitored, acetone, hexanal and formaldehyde presented the highest emission rates, with values exceeding 280 µg.m^{-2}.h^{-1}; the emission rates for other VOCs were less than 75 µg.m^{-2}.h^{-1}. According to our data (Figure 7), the air velocity over the PB surface did not significantly affect emission rates for the eight VOCs monitored.

In contrast to these results, some publications, such as Hun et al. (2010), suggested that the air velocity over the material's surface could affect VOC emission. An increase in the air velocity would have affected VOC emissions if they were mainly controlled by the convective mass transfer across the boundary layer (Knudsen et al., 1999). The VOC emissions measured here with the selected PB can hence be considered mainly influence by diffusion within the solid material. The VOC emission from the solid materials has a variable sensitivity to the air velocity over the material's surface depending on the predominant mechanism specific to each VOC-material pair.

3.1.7. Specific influence of the ACR on VOC emission rates

The influence of the ACR on VOC emissions from PB is illustrated in Figure 8. The emission rates for VOCs were measured in the chamber under different ACR while applying a constant air velocity over the material's surface.

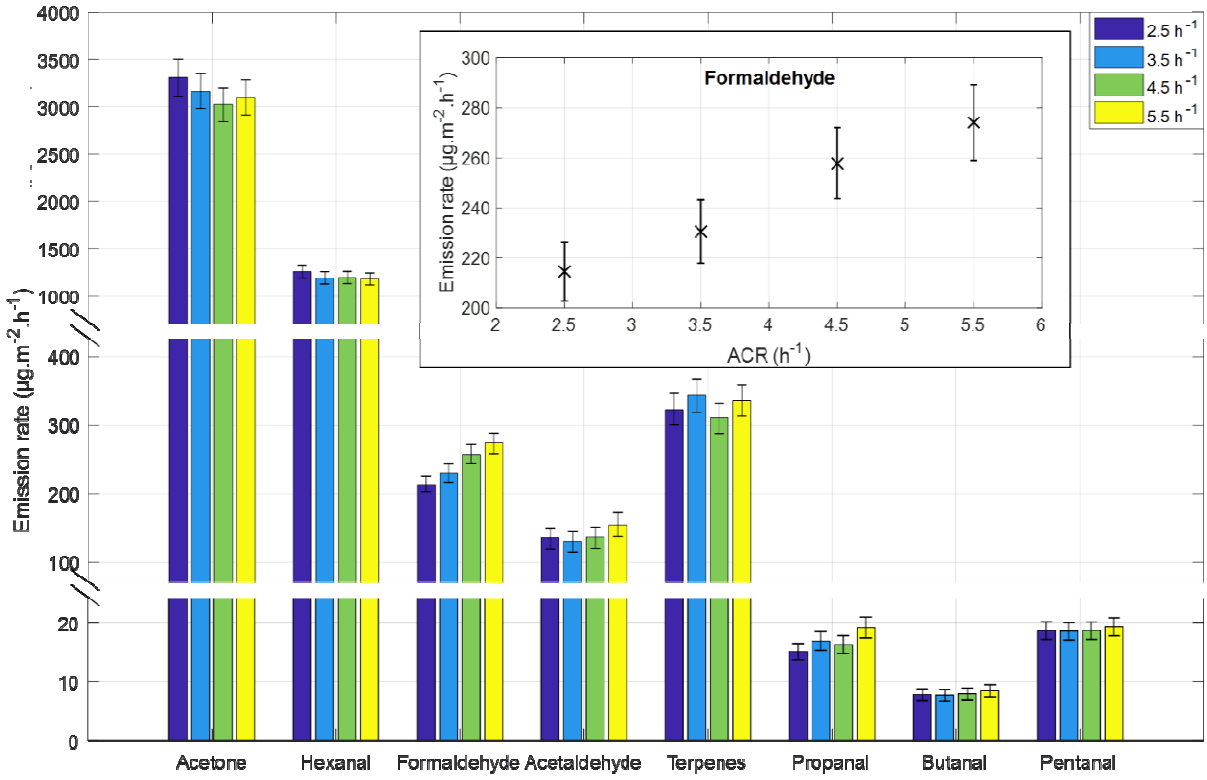

Figure 8. Emission rate (µg.m^{-2}.h^{-1}) for the eight main VOCs under different ACR (h^{-1}) conditions. Inset: emission rates for formaldehyde as a function of the ACR. Uncertainties correspond to the standard deviation calculated from the steady state concentrations measured.

As reported in Figure 8, the emission rates for seven VOCs were not significantly affected by changes to the ACR. In contrast, the formaldehyde emission rate increased by 28 % when the ACR varies from 2.5 to 5.5 h^{-1} that is significantly different compared to the variability between samples (7.1%). Propanal emission rates also showed a slight tendency to increase with the ACR, but overall emission rates remained lower than most other VOCs (< 20 µg.m^2.h^{-1}). These results highlight the singular behaviour of formaldehyde regarding the ACR. An increase in ACR means that more fresh air is brought into the chamber. Since the

553 air velocity close to the emissive material was constant, this should create a stronger
554 concentration gradient across the boundary layer (Offermann and Hodgson, 2011).

555 As discussed above, the influence of air velocity on VOC emission rates suggests that VOC
556 emissions from the selected PB, for the VOCs monitored, is mainly driven by their diffusion
557 within the solid material. Unlike the other VOCs, formaldehyde emission was enhanced by
558 increasing the concentration gradient from the material to the gas-phase, suggesting that
559 formaldehyde emission is not limited by its diffusion in the material.

560 Indeed, in addition to diffusing within the material, formaldehyde may be generated by
561 hydrolysis of the PB binder, which could explain it enhanced emission rate as the ACR
562 increases. Most composite wood panels are known sources of formaldehyde, as they are
563 bonded with urea-formaldehyde (UF) resins (Kelly et al., 1999; Salthammer et al., 2010).
564 These resins have a low resistance to hydrolysis (Dunky, 1998; Salthammer et al., 2010) as
565 a result of the reversibility of the reaction between urea and formaldehyde (Dorieh et al.,
566 2019). Thus, the C-N bond in UF resins can be hydrolyzed in the presence of water vapour
567 (Salthammer et al., 2010). This chemical process results in the release of free formaldehyde
568 which contributes to the total formaldehyde emission from composite wood panels (He et al.,
569 2019). Moreover, He et al. (2019) report that binder hydrolysis to produce formaldehyde
570 emission increases over time, becoming the predominant source of long-term emissions. In
571 our experiments, the supply of humid fresh air appears to promote the hydrolysis of the
572 binder and the formation of formaldehyde. However, the contribution of this process should
573 be limited in our conditions, since the emission phenomena are regarded as short-term.

574 **3.2. Material scale investigation**

575 In contrast to the previous series of tests, each experimental protocol alternately analysing
576 airtight/ventilated emission lasted for a full week. Over the course of these experiments,
577 temperature varied in line with day-night cycles, with fluctuations from 20 to 25 °C. Maximum
578 temperatures were measured during the day due to sunlight.

To account for these variations, a data correction was applied to concentration profiles using Equation 8, considering an identical influence of temperature on VOC emission in both steady state and transient conditions.

$$C_{corr,i} = C_{exp,i} + \alpha_i C_{exp,i}(T_{ref} - T_{exp}) \quad (Equation\ 8)$$

In Equation 8, $C_{corr,i}$ is the temperature corrected concentration (ppb) of VOC i, $C_{exp,i}$ is the experimental concentration (ppb) of VOC i, T_{ref} is the reference temperature set at 21 °C, T_{exp} is the experimental temperature and α_i is the relative concentration enhancement of VOC i per degree Celsius, as described in Equation 2. Concentration profiles for VOCs were corrected for temperature variations using Equation 2 and Equation 8, setting a reference temperature of 21 °C.

After performing the airtight/ventilated alternately emission experiments, corrected VOC concentrations were plotted. Figure 9 shows the examples of terpenes and formaldehyde. In this figure, the terpene concentration dynamic illustrates the behaviour of all targeted VOCs except formaldehyde, which was therefore represented separately.

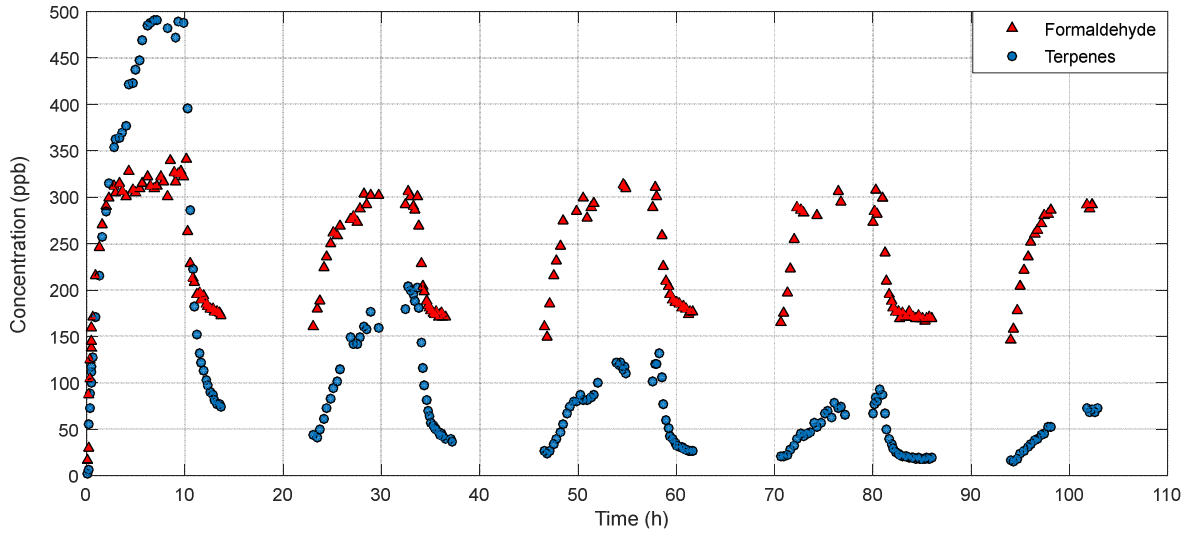

Figure 9. Comparison of the experimental concentration profiles for formaldehyde and terpenes (representing all other VOCs) (ppb).

All the experimental concentration profiles for VOCs were in agreement with the theoretical profiles shown in Figure 3. Figure 9 reveals two types of individual behaviour characterizing so-called 'rapid' and 'slow' kinetics, illustrated by formaldehyde and terpenes, respectively.

With the exception of formaldehyde, all VOCs presented similar emission kinetics, with from 5 to 15 h required to reach the steady state under airtight conditions. In addition, when switching from the airtight to the ventilated regime, a sharp decrease in concentration was observed with an average concentration drop exceeding 80% between the two regimes. The steady state concentration of terpenes under airtight conditions decreased from 490 to 75 ppb within less than 4 h of switching from the airtight to the ventilated condition.

In contrast, the concentration difference for formaldehyde between the airtight and ventilated regimes was lower than for other VOCs, with an average concentration drop of 45%. Noticeably, under ventilated conditions, formaldehyde maintained a concentration of ca. 175 ppb throughout the experimental sequence. Similarly, under the airtight regime, the steady state concentrations of formaldehyde were equivalent from one series of measurements to the next. In contrast, the steady state concentrations of other VOCs gradually decreased as time progressed.

Thus, compared to other VOCs, formaldehyde presents a singular behaviour in response to the ventilation regimes tested. This behaviour is in line with the results from the chamber scale approach. These findings suggest that the mechanisms driving formaldehyde emission could be quite different to those driving emission of the other VOCs monitored, as discussed above in relation to binder hydrolysis.

3.2.1. Determining K_i and $C_{0,i}$ by linear fitting

To determine the partitioning coefficient K_i and the initial emittable concentration $C_{0,i}$, the experimental data for the three experiments was fitted with a linear function. Experimental partitioning coefficients are reported in Table 3; Table 4 lists initial emittable concentrations.

621 Uncertainties correspond to the standard deviation (SD) calculated from the three
622 independent experiments.

623 **Table 3. Partitioning coefficient K_i of VOCs and associated standard deviation (SD) determined**
624 **from three experiments performed under the same conditions.**

K_i	Formaldehyde	Acetone	Acetaldehyde	Propanal	Butanal	Pentanal	Hexanal	Terpenes
Experiment 1	4380	211	180	193	312	273	313	113
Experiment 2	4404	212	180	206	355	317	316	109
Experiment 3	3184	225	198	267	357	305	287	110
SD (%)	17.5	3.7	5.6	17.8	7.5	7.5	5.3	2.1

625 All VOCs except formaldehyde had partitioning coefficients within the same order of
626 magnitude. A considerably higher partitioning coefficient was measured for formaldehyde.
627 Depending on the nature of the VOC, published values for the partitioning coefficients K_i
628 varied from one hundred to several thousand (Xu and Zhang, 2011; Zhou et al., 2018).
629 However, the partitioning coefficient values for formaldehyde presented here are consistent
630 with results reported elsewhere (S. Huang et al., 2013; Xu and Zhang, 2011; Zhou et al.,
631 2018).

632 For most of the VOCs investigated, uncertainties related to the partitioning coefficient were
633 lower than 7.5%. Thus, acetone, acetaldehyde, hexanal, and terpenes had a lower SD than
634 the corresponding measurement uncertainties, and uncertainties related to the variability
635 between samples. Consequently, the partitioning coefficients determined for these VOCs are
636 replicable. In contrast, the SD for butanal and pentanal were higher than the uncertainties
637 related to the variability between samples, but lower than their measurement uncertainties.
638 The uncertainties associated with the determination of their partitioning coefficients for these
639 VOCs are thus mostly related to analytical uncertainties.

640 Among the VOCs monitored, formaldehyde and propanal were the most variable compounds
641 with respective uncertainties of 17.5 and 17.8%. Nonetheless, these uncertainties remain
642 within the acceptable range.

643 Analysis of VOC depletion from the selected PB, characterized by the depletion rates,
644 revealed that it tended to decrease when the partitioning coefficient increased. Thus,
645 formaldehyde presented the highest partitioning coefficients (>3000) and the lowest depletion
646 rate compared to other VOCs, and conversely, VOCs which had low partitioning coefficients
647 (100 – 225), such as acetone, acetaldehyde, and terpenes, presented the highest depletion
648 rates.

649 Under ventilated conditions, the continuous flushing of the air volume eliminates gas-phase
650 VOC from the chamber, which sustains the VOC mass transfer from the material to the air,
651 controlled by the partitioning coefficient K_i. VOC depletion thus occurs, leading to a gradual
652 decrease in the concentration of the compound as the emission process progresses. For
653 compounds with a high K_i,such as formaldehyde, the relative concentration difference
654 between the air and the material is also high. Consequently, the amount of VOC removed
655 from the air of the chamber is low compared to the amount of VOC present within the PB,
656 which implies a limited depletion phenomenon and a low depletion rate. In contrast, for
657 compounds with a low K_i, the relative concentration difference between the air and the
658 material is also low. In these cases, the amount of VOC eliminated with the air from the
659 chamber is significant compared to the amount of VOC contained in the PB, resulting in
660 notable depletion and a high depletion rate.

661 **Table 4. Initial emittable concentration $C_{0,i}$ ($mg.m^{-3}$) of VOCs and associated standard deviation**
662 **(SD) determined from the three series of experiments performed under the same conditions.**

$C_{0,i}$	Formaldehyde	Acetone	Acetaldehyde	Propanal	Butanal	Pentanal	Hexanal	Terpenes
Experiment 1	1545	2484	105	22.6	12.4	33.7	2261	354
Experiment 2	1729	3188	127	28.2	15.9	43.6	2611	409
Experiment 3	1257	3988	119	21.1	14.7	40.5	2270	411
SD (%)	15.7	23.4	9.3	15.6	12.3	12.8	8.4	8.3

663 Formaldehyde, acetone and hexanal had the highest initial emittable concentrations in our
664 sample $C_{0,i}$ (>1200 $mg.m^{-3}$), whereas other VOCs presented $C_{0,i}$ of less than 420 $mg.m^{-3}$. Our
665 initial emittable concentrations $C_{0,i}$ agree with literature data (S. Huang et al., 2013; Zhou et

al., 2018). However, it should be noted that literature data for $C_{0,i}$ are spread over very broad ranges, since the initial emittable concentration depends on the type of material and its history. History of material correspond to combination of events occurring, storage duration and environmental conditions to which materials are subjected between manufacture and acquisition. For instance, formaldehyde presents an average initial emittable concentration of 17,000 mg.m^{-3} with an SD of 100% for different building materials (S. Huang et al., 2013; Zhou et al., 2018). Although the VOCs monitored presented uncertainties related to the determination of $C_{0,i}$ that were higher than those for the partitioning coefficient K_i, their respective uncertainties remained less than 23.4 %.

3.2.2. Determining D_i by solving of analytical equations

After determining K_i and $C_{0,i}$, the diffusion coefficient D_i was calculated by solving the analytical equation for the gas-phase VOC concentration in the airtight mode (Xiong et al., 2011). The VOC diffusion coefficients within the solid material D_i were determined by fitting the result of the solution of the analytical equation and the first experimental concentration profile under airtight conditions. VOC diffusion coefficients D_i determined from each experiment are reported in Table 5.

Table 5. Diffusion coefficients D_i (m^2.s^{-1}) for VOCs determined from the three experiments performed under the same conditions.

D_i (m^2.s^{-1})	Formaldehyde	Acetone	Acetaldehyde	Propanal	Butanal	Pentanal	Hexanal	Terpenes
Experiment 1	2.5x10^{-8}	3.0x10^{-9}	5.0x10^{-9}	2.0x10^{-9}	1.5x10^{-9}	1.5x10^{-9}	3.0x10^{-9}	8.0x10^{-8}
Experiment 2	2.5x10^{-8}	3.0x10^{-9}	4.0x10^{-9}	3.0x10^{-9}	1.0x10^{-9}	1.5x10^{-9}	3.0x10^{-9}	5.0x10^{-8}
Experiment 3	3.0x10^{-8}	1.5x10^{-9}	2.0x10^{-9}	1.5x10^{-9}	1.0x10^{-9}	1.0x10^{-9}	1.0x10^{-9}	2.0x10^{-9}
SD (%)	10.8	34.6	41.7	35.3	24.7	21.7	49.5	89.4

VOC diffusion within the solid material depends on the porosity of the material and on the nature of the given VOC. The extensive diversity of building materials studied in the literature results in D_i values ranging from 1.0x10^{-10} to 1.0x10^{-6} m^2.s^{-1} (S. Huang et al., 2013; Xu and Zhang, 2011). According to the results presented in Table 6, formaldehyde had the highest diffusion coefficient, with values ranging from 2.5x10^{-8} to 3.0x10^{-8} m^2.s^{-1}, which is in

689 agreement with published data (Xiong et al., 2008). The diffusion coefficients determined for
690 other VOCs varied from $1.0x10^{-9}$ to $5.0x10^{-9}$ $m^2.s^{-1}$.

691 Apart from terpenes, for which variable diffusion coefficient values were measured, with an
692 SD of 89.4%, the diffusion coefficients measured in the three experiments for all VOCs were
693 quite similar, with SD of less than 49.5%. The results for terpenes could be explained by their
694 higher variability between PB samples compared to other VOCs. Indeed, variations in
695 terpene emission rates between PB samples would significantly affect the first concentration
696 profile under the airtight conditions used to determine the diffusion coefficient D_i, resulting in
697 more scattered diffusion coefficient values for terpenes.

698 According to the data presented in Table 5, formaldehyde once again differs from the other
699 VOCs monitored. Based on the results of this study, the enhanced formaldehyde emission
700 rate as a function of the ACR could be explained by the following three hypotheses: (i)
701 Subject to the dynamic equilibrium concentration between the material and the air, the VOC
702 mass transfer needs to be strengthened if we are to satisfy this balance when the ACR
703 increases. As VOC emissions from the PB appears to be mainly driven by their diffusion
704 within the solid material, the diffusion process must contribute to formaldehyde emission
705 differently compared to the other VOCs monitored. In the case of formaldehyde, its high
706 diffusion within the material allows a continuous supply to reach the material's surface. In
707 contrast, the material's surface is less supplied with other VOCs due to their slower diffusion
708 within the solid material. Given the low rate of transport of VOCs to the material's surface by
709 diffusion, the amount of VOCs emitted from the material-air interface is limited. In this case,
710 the maximal emission capacity for VOC emission is restricted by the diffusive supply of VOC
711 and is not influenced by the ACR. In this scenario, diffusion of the VOC within the solid
712 material is the phenomenon limiting emission from the material studied. (ii) For all VOCs
713 monitored, including formaldehyde, diffusion within the solid material is the phenomenon
714 limiting emissions. The enhanced formaldehyde emission rate when the ACR increases
715 could be explained by hydrolysis of binding resin leading to the release of formaldehyde (He

et al., 2019). This hydrolysis may be promoted by the water present in the fresh air entering the chamber. Formaldehyde formation as a result of resin hydrolysis would continuously supply formaldehyde for emission (C_0), especially at the material's surface. (iii) A combination of the two previous hypotheses – formaldehyde diffusion within the material is high supplying the material's surface, and the PB resin is continuously hydrolysed to generate formaldehyde – could explain the enhanced formaldehyde emission rate in the high ACR conditions.

Although the analytical equation was solved for an airtight chamber, the convective mass transfer coefficient through the boundary layer h_i appears in the equation, since the mixing fan induced a convective airflow inside the chamber. However, some difficulties in the determination of D_i were encountered due to an unrealistic convective mass transfer coefficient. This parameter did not provide a satisfactory correlation between the experimental curve and the solution to the analytical equation. Axley (1991) indicates that the convective mass transfer coefficient h_i can be calculated using theoretical equations based on ideal cases. These equations mainly depend on two unreliable parameters: the mean fluid velocity near to the material's surface (U) and the length of the surface in the direction of the flow (L). U and L can vary considerably from one case to another. Therefore, the convective mass transfer coefficients must be calculated once again using U and L values that agree better with all the VOCs studied from Equation 3. In this paper, h_i only depended on the molecular diffusivity of the VOCs in air. All convective mass transfer coefficients are reported in Table 6.

Table 6: Convective mass transfer coefficients h_i for the eight VOCs emitted from the selected PB ($m.s^{-1}$).

i	Formaldehyde	Acetone	Acetaldehyde	Propanal	Butanal	Pentanal	Hexanal	Terpenes
h_i ($m.s^{-1}$)	$1.61x10^{-4}$	$1.26x10^{-4}$	$1.26x10^{-4}$	$1.12x10^{-4}$	$1.01x10^{-4}$	$9.41x10^{-5}$	$8.84x10^{-5}$	$7.66x10^{-5}$

According to several publications (Zhang and Niu, 2004, 2003; Zhang et al., 2018, 2003), convective mass transfer usually varies from $1.0x10^{-4}$ to $1.0x10^{-2}$ $m.s^{-1}$ for building materials. Compared to published h_i values, the VOCs emitted from our PB present low convective

742 mass transfer coefficients (Table 6). Since convective mass transfer through the boundary
743 layer is affected by the airflow over the material surface, especially its velocity, the low h_i
744 values could explain the negligible impact of the air velocity over the material's surface on
745 VOC emissions reported above. These low convective mass transfer coefficients corroborate
746 the hypothesis that VOC emissions from the PB studied here are mainly controlled by their
747 diffusion within the material.

748 If Equation 3 is reworked to a different form using Equation 5, the positive correlation
749 between the convective mass transfer coefficients h_i and the molecular diffusion in air δ_i can
750 be highlighted. Since molecular diffusion in air is negatively correlated with molar weight
751 according to Equation 6, it results in negative correlation relationship between the coefficient
752 h_i and molar weight. Thus, it can be observed that the convective mass transfer coefficient h_i
753 is negatively correlated with the molar weight of VOCs. Among the VOCs monitored,
754 formaldehyde had the lowest molar weight, at 30.03 $g.mol^{-1}$ and the highest convective mass
755 transfer coefficient. Conversely, terpenes had the lowest convective mass transfer coefficient
756 and the highest molar weight (136.24 $g.mol^{-1}$).

757 **4. Conclusion**

758 With a view to reducing VOC concentrations in indoor environments, ventilation is known to
759 have a significant effect on VOC emissions. However, ventilation could differentially affect
760 the behaviour of individual VOCs emitted from a single solid material. To understand the
761 physical phenomenon of VOC emission, in this study, the individual behaviours of VOCs
762 were assessed using two distinct scales of study. Firstly, the respective impacts of air
763 velocity and the ACR on VOC emissions were measured. This overall assessment of the
764 influence of ventilation highlighted the non-conformist behaviour of formaldehyde with
765 respect to the ACR even through changes to the speed of the air flowing over the material's
766 surface did not significantly alter the emission rates for any of the VOCs studied. By
767 determining the key emission parameters (K_i, $C_{0,i}$, D_i) for the VOCs studied, we discovered
768 that formaldehyde had higher partitioning and diffusion coefficients than the other

compounds. These significant differences in diffusion and partitioning coefficients between formaldehyde and other VOCs allowed us to propose physical interpretations of the data related to the specific influence of the ACR on the formaldehyde emission rate. VOC emissions are mainly controlled by the VOC's diffusion within the material, which is the limiting process in VOC emission for our solid material. When the ACR increased, the formaldehyde emission rate was enhanced due to its higher diffusion and partitioning coefficients compared to other VOCs. A detailed sensitivity analysis of the experimental method should be carried out to assess the quality of the data obtained. This analysis would be worth a full paper.

The influence of environmental parameters on VOC emissions will need to be further investigated as temperature has been observed to have a significant effect on overall VOC emissions at chamber scale. The influence of the environmental conditions (temperature and RH) on key emission parameters (K_i, $C_{0,i}$, D_i) should then be assessed at material scale. Since the impact of environmental parameters on emission parameters has not been extensively documented, with data only available for formaldehyde, relationships between environmental parameters and each emission parameters could be proposed for several VOCs emitted from a single solid material.

This paper provides new insight into the mechanisms governing VOC emissions. Moreover, some VOCs were shown to display unique behaviour with respect to ventilation, in particular formaldehyde. This observation underlines the need to individually consider the VOCs monitored when investigating their emission rates from solid materials in indoor environments. Finally, the enhanced formaldehyde emission rate as a function of the ACR calls for care to be taken and for the singular behaviour of formaldehyde to be considered when establishing indoor air quality prevention strategies based on ventilation.

Acknowledgements

This work was achieved in the frame of ESQUISSE project, funded by INRS. It results from a collaboration between INRS and IMT Lille Douai. Florent Caron acknowledges INRS for funding his PhD.

References

Axley, J.W., 1991. Adsorption Modelling for Building Contaminant Dispersal Analysis. Indoor Air 1, 147–171. https://doi.org/10.1111/j.1600-0668.1991.04-12.x

Bodalal, A., Zhang, J.S., Plett, E.G., 2000. A method for measuring internal diffusion and equilibrium partition coefficients of volatile organic compounds for building materials. Building and Environment 10.

Colombo, A., De Bortoli, M., Knoppel, H., Pecchio, E., Vissers, H., 1993. Adsorption Of Selected Volatile Organic Compounds On A Carpet, A Wall Coating, And A Gypsum Board In A Test Chamber. Indoor Air 3, 276–282. https://doi.org/10.1111/j.1600-0668.1993.00009.x

Cox, S.S., Liu, Z., Little, J.C., Howard-Reed, C., Nabinger, S.J., Persily, A., 2010. Diffusion-controlled reference material for VOC emissions testing: proof of concept. Indoor Air 20, 424–433. https://doi.org/10.1111/j.1600-0668.2010.00666.x

de Gennaro, G., de Gennaro, L., Mazzone, A., Porcelli, F., Tutino, M., 2014. Indoor air quality in hair salons: Screening of volatile organic compounds and indicators based on health risk assessment. Atmospheric Environment 83, 119–126. https://doi.org/10.1016/j.atmosenv.2013.10.056

Dorieh, A., Mahmoodi, N.O., Mamaghani, M., Pizzi, A., Mohammadi Zeydi, M., moslemi, A., 2019. New insight into the use of latent catalysts for the synthesis of urea formaldehyde adhesives and the mechanical properties of medium density fiberboards bonded with them. European Polymer Journal 112, 195–205. https://doi.org/10.1016/j.eurpolymj.2019.01.002

Dunky, M., 1998. Urea–formaldehyde (UF) adhesive resins for wood. International Journal of Adhesion and Adhesives 18, 95–107. https://doi.org/10.1016/S0143-7496(97)00054-7

822 Fuller, E.N., Ensley, K., Giddings, J.C., 1969. Diffusion of halogenated hydrocarbons in
823 helium. The effect of structure on collision cross sections. The Journal of Physical
824 Chemistry 73, 3679–3685. https://doi.org/10.1021/j100845a020
825 Fuller, E.N., Giddings, J.C., 1965. A Comparison of Methods for Predicting Gaseous
826 Diffusion Coefficients. Journal of Chromatographic Science 3, 222–227.
827 https://doi.org/10.1093/chromsci/3.7.222
828 Fuller, E.N., Schettler, P.D., Giddings, J.Calvin., 1966. NEW METHOD FOR PREDICTION
829 OF BINARY GAS-PHASE DIFFUSION COEFFICIENTS. Industrial & Engineering
830 Chemistry 58, 18–27. https://doi.org/10.1021/ie50677a007
831 Harb, P., Locoge, N., Thevenet, F., 2018. Emissions and treatment of VOCs emitted from
832 wood-based construction materials: Impact on indoor air quality. Chemical
833 Engineering Journal 354, 641–652. https://doi.org/10.1016/j.cej.2018.08.085
834 He, Z., Xiong, J., Kumagai, K., Chen, W., 2019. An improved mechanism-based model for
835 predicting the long-term formaldehyde emissions from composite wood products with
836 exposed edges and seams. Environment International 132, 105086.
837 https://doi.org/10.1016/j.envint.2019.105086
838 Huang, L., Mo, J., Sundell, J., Fan, Z., Zhang, Y., 2013. Health Risk Assessment of
839 Inhalation Exposure to Formaldehyde and Benzene in Newly Remodeled Buildings,
840 Beijing. PLOS ONE 8, e79553. https://doi.org/10.1371/journal.pone.0079553
841 Huang, S., Wei, W., Weschler, L.B., Salthammer, T., Kan, H., Bu, Z., Zhang, Y., 2017. Indoor
842 formaldehyde concentrations in urban China: Preliminary study of some important
843 influencing factors. Science of The Total Environment 590–591, 394–405.
844 https://doi.org/10.1016/j.scitotenv.2017.02.187
845 Huang, S., Xiong, J., Zhang, Y., 2013. A rapid and accurate method, ventilated chamber C-
846 history method, of measuring the emission characteristic parameters of
847 formaldehyde/VOCs in building materials. Journal of Hazardous Materials 261, 542–
848 549. https://doi.org/10.1016/j.jhazmat.2013.08.001

Huangfu, Y., Lima, N.M., O'Keeffe, P.T., Kirk, W.M., Lamb, B.K., Pressley, S.N., Lin, B., Cook, D.J., Walden, V.P., Jobson, B.T., 2019. Diel variation of formaldehyde levels and other VOCs in homes driven by temperature dependent infiltration and emission rates. Building and Environment 159, 106153. https://doi.org/10.1016/j.buildenv.2019.05.031

Hult, E.L., Willem, H., Price, P.N., Hotchi, T., Russell, M.L., Singer, B.C., 2015. Formaldehyde and acetaldehyde exposure mitigation in US residences: in-home measurements of ventilation control and source control. Indoor Air 25, 523–535. https://doi.org/10.1111/ina.12160

Hun, D.E., Corsi, R.L., Morandi, M.T., Siegel, J.A., 2010. Formaldehyde in Residences: Long-Term Indoor Concentrations and Influencing Factors. Indoor Air. https://doi.org/10.1111/j.0905-6947.2010.00644.x

Kelly, T.J., Smith, D.L., Satola, J., 1999. Emission Rates of Formaldehyde from Materials and Consumer Products Found in California Homes 8.

Knudsen, H.N., Kjaer, U.D., Nielsen, P.A., Wolkoff, P., 1999. Sensory and chemical characterization of VOC emissions from building products: impact of concentration and air velocity. Atmospheric Environment 33, 1217–1230. https://doi.org/10.1016/S1352-2310(98)00278-7

Liu, Z., Howard-Reed, C., Cox, S.S., Ye, W., Little, J.C., 2014. Diffusion-controlled reference material for VOC emissions testing: effect of temperature and humidity. Indoor Air 24, 283–291. https://doi.org/10.1111/ina.12076

Liu, Z., Ye, W., Little, J.C., 2013. Predicting emissions of volatile and semivolatile organic compounds from building materials: A review. Building and Environment 64, 7–25. https://doi.org/10.1016/j.buildenv.2013.02.012

Myers, G.E., 1982. Formaldehyde dynamic air contamination by hardwood plywood: effects of several variables and board treatments. Forest products journal 32, 20–25.

Nirlo, E.L., Crain, N., Corsi, R.L., Siegel, J.A., 2014. Volatile organic compounds in fourteen U.S. retail stores. Indoor Air 24, 484–494. https://doi.org/10.1111/ina.12101

877 Offermann, F.J., Hodgson, A.T., 2011. Emission Rates of Volatile Organic Compounds in
878 New Homes 7.
879 Risholm-Sundman, M., 1999. Determination of Formaldehyde Emission with Field and
880 Laboratory Emission Cell (FLEC) - Recovery and Correlation to the Chamber Method.
881 Indoor Air 9, 268–272. https://doi.org/10.1111/j.1600-0668.1999.00006.x
882 Robert, L., Guichard, R., Klingler, J., Cochet, V., 2018. IMPACT OF VENTILATION ON
883 INDOOR AIR QUALITY IN A SPORTS STORE 7.
884 Salthammer, T., Mentese, S., Marutzky, R., 2010. Formaldehyde in the Indoor Environment.
885 Chemical Reviews 110, 2536–2572. https://doi.org/10.1021/cr800399g
886 Shang, Y., Li, B., Baldwin, A.N., Ding, Y., Yu, W., Cheng, L., 2016. Investigation of indoor air
887 quality in shopping malls during summer in Western China using subjective survey
888 and field measurement. Building and Environment 108, 1–11.
889 https://doi.org/10.1016/j.buildenv.2016.08.012
890 Smith, J.F., Gao, Z., Zhang, J.S., Guo, B., 2009. A New Experimental Method for the
891 Determination of Emittable Initial VOC Concentrations in Building Materials and
892 Sorption Isotherms for IVOCs. CLEAN – Soil, Air, Water 37, 454–458.
893 https://doi.org/10.1002/clen.200900003
894 Tiffonnet, A.-L., 2000. Contribution à l'analyse de la Qualité de l'Air Intérieur: Influence des
895 transports de Composés Organiques Volatils (COV) entre les parois et l'ambiance
896 (PhD Thesis). La Rochelle.
897 Tiffonnet, A.-L., Marion, M., Makhloufi, R., Blondeau, P., 2006. Etude des résistances au
898 transfert de COV entre une paroi et l'ambiance 9.
899 Uhde, E., Borgschulte, A., Salthammer, T., 1998. Characterization of the field and laboratory
900 emission cell—FLEC: Flow field and air velocities. Atmospheric Environment 32, 773–
901 781. https://doi.org/10.1016/S1352-2310(97)00345-2
902 Wolkoff, P., 1998. Impact of air velocity, temperature, humidity, and air on long-term voc
903 emissions from building products. Atmospheric Environment 32, 2659–2668.
904 https://doi.org/10.1016/S1352-2310(97)00402-0

905 Wolkoff, P., Nielsen, G.D., 2001. Organic compounds in indoor air—their relevance for
906 perceived indoor air quality? Atmospheric Environment 35, 4407–4417.
907 Xiong, J., Zhang, Y., Huang, S., 2011. Characterisation of VOC and Formaldehyde Emission
908 from Building Materials in a Static Environmental Chamber: Model Development and
909 Application: Indoor and Built Environment.
910 https://doi.org/10.1177/1420326X103874801
911 Xiong, J., Zhang, Y., Wang, X., Chang, D., 2008. Macro–meso two-scale model for predicting
912 the VOC diffusion coefficients and emission characteristics of porous building
913 materials. Atmospheric Environment 42, 5278–5290.
914 https://doi.org/10.1016/j.atmosenv.2008.02.062
915 Xu, J., Zhang, J.S., 2011. An experimental study of relative humidity effect on VOCs'
916 effective diffusion coefficient and partition coefficient in a porous medium. Building
917 and Environment 46, 1785–1796. https://doi.org/10.1016/j.buildenv.2011.02.007
918 Yoon, H.I., Hong, Y.-C., Cho, S.-H., Kim, H., Kim, Y.H., Sohn, J.R., Kwon, M., Park, S.-H.,
919 Cho, M.-H., Cheong, H.-K., 2010. Exposure to volatile organic compounds and loss of
920 pulmonary function in the elderly. European Respiratory Journal 36, 1270–1276.
921 https://doi.org/10.1183/09031936.00153509
922 Zhang, L.Z., Niu, J.L., 2004. Modeling VOCs emissions in a room with a single-zone multi-
923 component multi-layer technique. Building and Environment 39, 523–531.
924 https://doi.org/10.1016/j.buildenv.2003.10.005
925 Zhang, L.Z., Niu, J.L., 2003. Laminar fluid flow and mass transfer in a standard field and
926 laboratory emission cell. International Journal of Heat and Mass Transfer 10.
927 Zhang, X., Cao, J., Wei, J., Zhang, Y., 2018. Improved C-history method for rapidly and
928 accurately measuring the characteristic parameters of formaldehyde/VOCs emitted
929 from building materials. Building and Environment 143, 570–578.
930 https://doi.org/10.1016/j.buildenv.2018.07.030
931 Zhang, Y., Deng, Q., Qian, H., Mo, J., 2012. Research advance report of indoor environment
932 and health in China. China Architecture & Building PressChina.

933 Zhang, Y., Yang, R., Zhao, R., 2003. A model for analyzing the performance of photocatalytic
934 air cleaner in removing volatile organic compounds. Atmospheric Environment 37,
935 3395–3399. https://doi.org/10.1016/S1352-2310(03)00357-1
936 Zhou, X., Liu, Y., Liu, J., 2018. Alternately airtight/ventilated emission method: A universal
937 experimental method for determining the VOC emission characteristic parameters of
938 building materials. Building and Environment 130, 179–189.
939 https://doi.org/10.1016/j.buildenv.2017.12.025